

# Fiber Optic Chemical Sensors based on Single-Walled Carbon Nanotubes: Perspectives and Challenges

Marco Consales<sup>1</sup>, Antonello Cutolo<sup>1</sup>, Michele Penza<sup>2</sup>, Patrizia Aversa<sup>2</sup>,  
Michele Giordano<sup>3</sup> and Andrea Cusano<sup>1</sup>

<sup>1</sup> *Optoelectronic Division, University of Sannio, Benevento, Italy*

<sup>2</sup> *Department of Physical Technologies and New Materials, ENEA, Brindisi, Italy*

<sup>3</sup> *Institute for Composite and Biomedical Materials, CNR, Portici, Italy*

## 1. Introduction

Carbon nanotubes (CNTs) have become a highly-studied material class in recent years for numerous applications in nanoscience and nanotechnology due to their outstanding physical and chemical properties. High chemical reactivity, excellent mechanical strength but ultra-light weight, high thermal stability, high electron mobility, rich electronic properties, high aspect ratio, hollow nanostructure, large surface area make CNTs an ideal platform for many nanomaterial micro/nano-systems and process control practical applications. Conceptually, carbon nanotubes are viewed as rolled-up structures at nanoscale into seamless cylinders of single or multiple sheets of graphene to engineering single-walled and coaxial multi-walled carbon nanotubes, respectively. Generally, the diameter of a single nanotube ranges from 1 to 5 nanometers; while the bundles of roped multiple nanotubes have a diameter varying in the range of 5-100 nm. These one-dimensional nanostructured carbon allotropes have been applying to explore their potential in chemical gas sensing and biosensing.

This chapter reviews the development of high performance opto-chemical sensors based on the integration of CNTs with the optical fiber technology. The paper starts with an overview of the CNT amazing features and their exploitation as highly adsorbent nano-scale materials for chemical sensing. The attention is then focused on the operating principle, fabrication and characterization of fiber optic chemo-sensors in the Fabry-Perot type reflectometric configuration, realized by means of the deposition of a thin sensitive layer of single-walled carbon nanotubes (SWCNTs)-based material on the distal end of standard silica optical fibers (SOFs). This is followed by an extensive review of the excellent room temperature sensing capabilities of the realized SWCNT sensors against Volatile Organic Compounds (VOCs) in different environments (air and water). The experimental results here reported reveal that ppm and sub-ppm chemical detection limits, low response times as well as fast and complete recovery of the sensor responses have been obtained in most of the investigated cases. This evidences the great potentialities of the proposed photonic sensors

based on SWCNTs and their feasibility to be successfully employed for practical environmental monitoring applications, both in vapor or liquid phase. Furthermore, the use of SWCNT-based nanocomposites as novel sensitive fiber coatings is proposed to enhance the chemical sensing performance and improve the adhesion of CNTs to the fiber surface. It will also be shown how the typical poor selectivity of SWCNTs-based sensors towards a given chemical specie can be overcome by using standard pattern recognition techniques applied to fiber optic sensor arrays, exploiting both the static and dynamical features of the single sensor responses.

## 2. Chemical sensors for environmental monitoring

Environmental monitoring is required to protect the public and the environment from toxic contaminants and pathogens that can be released into a variety of media including air, soil, and water. Air pollutants include sulfur dioxide, carbon monoxide, nitrogen dioxide, and VOCs, which originate from sources such as vehicle emissions, power plants, refineries, and industrial and laboratory processes. Soil and water contaminants can be classified as microbiological, radioactive, inorganic, synthetic organic, and VOCs. Pesticide and herbicides are applied directly to plants and soils, and incidental releases of other contaminants can originate from spills, leaking pipes, underground storage tanks, waste dumps, and waste repositories. Some of these contaminants can persist for many years and migrate through large regions of soil until they reach water resources, where they may present an ecological or human-health threat. The current monitoring methods are mainly based on off-site laboratory analyses and are costly and time-consuming. In addition, limitations in sampling and analytical techniques occur (Wilson et al., 1995; Looney and Falta, 2000). For this reason, a need exists for accurate, inexpensive, continuous and long-term monitoring of environmental contaminants using sensors that can be operated on site.

Chemical sensors can be in most cases schematically described as composed of a sensitive part which, interacting with the surrounding environment, collects and concentrate molecules at or within the surface undergoing physical changes, and of an opportune transducer that converts into an interpretable and quantifiable term such modification of the sensing part. The heart of the chemical sensor is the sensitive element which is the interface between transducer and external environment so that the nature, the selectivity and sensitivity of the sensor depends upon these interactive materials. Good materials to use as sensing part should optimize specific interactions with a target analyte or narrow class of analytes, should provide a fast and reversible diffusion of the penetrants, small recovery times and should maintain the physical state so as the geometry over several cycles of use, in order to avoid hysteretic effects, and thus to ensure the reproducibility (Grate & Abram, 1991). Candidate materials for chemical sensors include polymers, organic monolayers, ceramics, metals semiconductors, nanostructured and porous materials (nanomaterials, molecular sieves, sol-gels, aerogels), biomolecules and combination thereof.

The natural step following the selective recognition of an analyte from the sensitive layer is the signal transduction, and thus the choice of an opportune technique to read the physical or chemical changes occurring at the sensing part. Transducing approaches can include mechanical (acoustic wave, micromechanical), electrochemical, optical, thermal, and electronic types. Each has strengths and weaknesses relative to the particular application.

Each transduction principle can be implemented in a variety of configurations, and fabricated by multiple approaches, resulting in many different sensing platforms.

A number of chemical sensors have been developed for environmental monitoring applications, a classification of which can be carried out upon their principal physics and operating mechanisms. The most exploited transduction principles in chemical sensing are the mass change and the resistivity/conductivity change of the sensitive element occurring on exposure to and consequent sorption of molecules of target environmental analytes. The first physical parameter is in many cases measured by the shift in the resonant frequency of an oscillating piezoelectric crystal. Depending on the kind of vibrational wave propagated in the crystal, a mass sensor can be classified as Quartz Crystal Microbalance (QCM) or Surface Acoustic Wave (SAW) sensor (Hartman et al., 1994; Kepley et al., 1992; Penza et al., 2006\_a). They typically use a thin polymeric film as sensitive layer (Grate, 2000), however SAW and QCM-based chemical sensors using other sensitive coatings have been proposed (Zhang et al., 2004; Penza et al., 2005\_a). Instead, resistivity/conductivity changes are typically detected by conductometric measurement carried out on sensitive materials (mainly semiconducting metal oxides and conjugated polymers) deposited between two electrodes. These sensor technologies carry the name of Metal Oxide Semiconductors (MOS) and Conductive Organic Polymer (COP) sensors (James et al., 2005). During the last two decades, however, a remarkable interest has been also focused on optical transduction principles for the measurement of chemical and biological quantities (Baldini et al., 2006). A large variety of devices based on optical methods have been used in chemical sensing and biosensing including ellipsometry, spectroscopy (luminescence, phosphorescence, fluorescence, Raman), interferometry (white light interferometry, modal interferometry in optical waveguide structures), spectroscopy of guided modes in optical waveguide structures (grating coupler, resonant mirror), and surface plasmon resonance (Wolfbeis, 2004; Zudans et al., 2004; Steinberg et al., 2003; Orellana, 2004; Homola et al., 1999; Mignani et al., 2005; Arregui et al., 2003; Brecht & Gauglitz, 1995; Gauglitz, 1996; Boisde, 1996). In these sensors a desired quantity is determined by measuring refractive index, absorbance and fluorescence properties of analyte molecules or of a chemo-optical transducing medium. Optical fiber sensors are also very attractive in chemical sensing applications due to some unique characteristics deriving by the use of optical fibers, one of the most outstanding characteristic of which is their ability to transmit light over large distances with low losses allowing a sensor head to be remotely located from the instrumentation. This feature is particularly useful for sensing in harsh environments where hazardous chemicals may be present or extremes in temperature occur. In addition the small size, light weight and high flexibility of fibres allow access to areas that would be otherwise difficult to reach.

Provided the optical power density are within certain limits, fiber optic chemical sensors are much safer in explosive environments compared with sensors involving electrical signals, where a spark may trigger a gas explosion. Optical signals are immune to electrical or magnetic interference from, for examples, power lines and electrical machinery. Furthermore optical fibers have the capability of carrying a huge amount of information, much greater than that carried by electrical wires. Fiber optic sensing is very versatile, since the intensity, wavelength, phase and polarization of light can all be exploited as measurement parameters, and several wavelengths launched in the same fiber in either direction form independent signals. This gives the possibility to monitor several chemicals with the same fiber sensor or even simultaneously monitor unwanted environment

parameter variations which could drastically affect the chemical concentration measurements, such as the temperature or disturbance of the fiber. Multiplexing of fiber optic systems is also relatively easy, allowing expensive source or analysis instrumentation to be shared among a number of sites.

This contribution reviews the integration of carbon nanotubes as advanced sensitive coatings with optical fiber technology for the development of high performance opto-chemical sensors exploitable for several environmental monitoring applications. In particular, the excellent sensing capabilities of the realized photonic chemo-sensors against VOCs and other pollutants in air and water, at room temperature, will be reviewed.

## **2.1 Carbon nanotubes: advanced materials for chemical sensing**

The search for new advanced materials is an important area of contemporary research in numerous disciplines of science. Great attention has been paid in recent years to nano-structured materials of different chemical composition, produced as nanoparticles, nanowires or nanotubes. Similarly, there has already been great interest in their preparation, properties and applications in the literature. As matter of fact, with the development of nano-science and nano-technology, a large number of literatures on one-dimensional nanostructured materials, including tubes, rods, belts, and wires in this area, have been published every year (Huang & Choi, 2007). These materials have their unique structures which are dominated by a wire-like structure whose diameter varies over a broad range from several tens of nanometers to a micrometer. In particular, carbon-based nanostructures exhibit unique properties and morphological flexibility, which renders them inherently multifunctional and compatible with organic and inorganic systems.

Carbon nanotubes (CNTs), discovered by Iijima in 1991 (Iijima, 1991) are at the forefront of the novel nanoscale investigations and nanostructure effects due to their unique electronic, chemical, structural, optical, mechanical and thermal properties depending on their specific hollow nanostructure with surface-arranged carbon atoms organized in rolled one-dimensional seamless tubes (Dresselhaus et al., 2001; Dai, 2002). They are considered as a new form of pure carbon, and can essentially be thought of as layers of graphite rolled-up into a tube to form a cylinder with diameter of few nanometers and length ranging from 1 to 100 microns. To date, CNTs are building blocks considered as the most promising functional nanomaterial for future miniaturized gas nanosensors due to their hollow nanostructure and high specific surface area which provide attractive characteristics for gas sensing applications. In fact, due to their unique morphology, CNTs possess the excellent capability to reversibly adsorb molecules of environmental pollutants undergoing a modulation of their electrical, geometrical and optical properties, such as conductivity, refractive index, thickness etc. CNTs can be distinguished in SWCNTs or multi-walled carbon nanotubes (MWCNTs) depending on whether only one layer or many layers of graphite are concentrically rolled up together, and can behave either as metallic or semiconducting, depending upon their diameter and chirality (the way the hexagons are arranged along the tubule axis) (Terrones, 2003). SWCNTs are a very important variety of carbon nanotube because they exhibit important electrical and sensing properties that are not shared by the MWCNTs variants. The purity of the CNTs affects their sensing performance, thus efficient purification protocols to remove metallic impurities and amorphous carbon particles have been developed as well (Penza et al., 2007\_a).

## 2.2 Chemical sensors based on carbon nanotubes: state of the art

The special geometry of carbon nanotubes and their characteristic of being all surface reacting materials offer great potential applications as chemical sensor devices with excellent sensitivities and fast responses (Riu et al., 2008). Most of the sensors based on CNTs are field effect transistors (FET), since much interest has been focused in the past on the study of the changes in their electrical properties as a consequence of the interaction with gaseous and VOC molecules: many studies have shown that although carbon nanotubes are robust and inert structures, their electrical properties are extremely sensitive to the effects of charge transfer and chemical doping by various molecules. The electronic structures of target molecules near the semiconducting nanotubes cause measurable changes to the nanotubes electrical conductivity. Nanosensors based on changes in electrical conductance are highly sensitive, but they are also limited by factors such as their inability to identify analytes with low adsorption energies, poor diffusion kinetics and poor charge transfer with CNTs (Modi et al., 2003).

Kong et al. (Kong et al., 2000) were probably the first to show that CNTs can be used in chemical sensors since exposing SWCNTs to electron withdrawing (e.g. NO<sub>2</sub>) or donating (e.g. NH<sub>3</sub>) gaseous molecules dramatically increases or decreases the electrical resistance of SWCNTs in the transistor scheme. In addition CNTs-based sensors demonstrated a fast response and a higher sensitivity than, for example, solid-state sensors at room temperature. More or less in the same period, it was demonstrated that the electrical conductance of SWCNTs could be modified in presence of O<sub>2</sub> (Collins et al., 2000). The effect of the adsorption of several gas compounds in SWCNTs was also described (Sumanasekera et al., 2000), as well as those of water vapor on the electrical resistance of a SWCNT (Zahab et al., 2000). Shortly afterwards, Fujiwara et al. (Fujiwara et al., 2001) studied the N<sub>2</sub> and O<sub>2</sub> adsorption properties of SWCNT bundles and their structures. All these studies opened the door to the development of chemical sensors based on CNTs.

Sensing devices based not only on the changes in the electrical properties of CNTs but also on other principles were proposed. For example, bundles of SWCNTs (Adu et al., 2001) have measured the thermoelectric qualitative response to a variety of gases (He, N<sub>2</sub>, H<sub>2</sub>, O<sub>2</sub> and NH<sub>3</sub>). Sumanasekera et al. (Sumanasekera et al., 2002) created a thermoelectric chemical sensor to measure the easily detectable and reversible thermoelectric power changes of SWCNTs when they are in contact with He, N<sub>2</sub> and H<sub>2</sub>. Chopra et al. (Chopra et al., 2003) developed a circular disk resonator coated with SWCNTs using a conductive epoxy, which selectively detects the qualitative presence of several gases (NH<sub>3</sub>, CO, Ar, N<sub>2</sub> and O<sub>2</sub>) due to changes in the dielectric constant and shifts in the resonant frequency.

Wei et al. (Wei et al., 2003) demonstrated a gas sensor depositing CNT bundles onto a piezoelectric quartz crystal. This sensor detected CO, NO<sub>2</sub>, H<sub>2</sub> and N<sub>2</sub> by detecting changes in oscillation frequency and was more effective at higher temperatures (200 °C). Penza et al. (Penza et al., 2004\_a) developed SAW and QCM sensor coated with SWCNTs and MWCNTs and used them to detect VOCs such as ethanol, ethylacetate and toluene by measuring the downshift in the resonance frequency of the acoustic transducers.

Carbon nanotubes can be easily functionalized with molecules enabling the specific interaction with target chemicals thus improving the typically low selectivity of CNTs-based devices. In this way, different types of sensors based on molecular recognition interactions can be developed, allowing the development of nanosensors that are highly selective and sensitive. Chen et al. (Chen et al., 2003) used a non-covalent functionalized FET based on

SWCNTs for selectively recognizing target proteins in solution. Azanian et al. (Azamian et al., 2002) immobilized glucose oxidase on SWCNTs and enhanced the catalytic signal by more than one order of magnitude compared to that of an activated macro-carbon electrode. Zhao et al. (Zhao et al., 2002) worked with horseradish peroxidase and Sotiropoulou et al. (Sotiropoulou et al., 2003) worked with enzymes. Barone et al. (Barone et al., 2002) developed a device for  $\beta$ -D-glucose sensing in solution phase. They also showed two distinct mechanisms of signal transduction: fluorescence and charge transfer.

Recently, further interest has also been devoted to the possibility to change the optical and/or geometrical properties of SWCNTs upon adsorption of target analyte molecules, enabling to exploit such materials for the development of opto-chemical sensors for numerous environmental monitoring application, from chemical detection in air and water (Consales et al., 2006\_a; Penza et al., 2004\_b; Penza et al., 2005\_b; Cusano et al., 2006\_a; Consales et al., 2007\_a) to hydrogen detection at cryogenic temperatures suitable for aerospace applications (Cusano et al., 2006\_b). In particular, the possibility of exploiting such materials in conjunction with the optical fiber technology could enable the development of optoelectronic noses and tongues capable of air and water quality monitoring, characterized by ppm and sub-ppm resolutions, good recovery features and fast responses, as it will be seen in section 4 and 5.

### 3. Opto-chemical sensors in reflectometric configuration

The reflectometric configuration is essentially based on a low finesse and extrinsic Fabry-Perot (FP) interferometer and, as schematically shown in Fig. 1, uses a thin sensitive film deposited at the distal end of a properly cut and prepared SOF to produce a FP cavity. The first mirror is given by the fiber/sensitive layer interface whereas the second one is given by the sensitive layer/external medium interface.

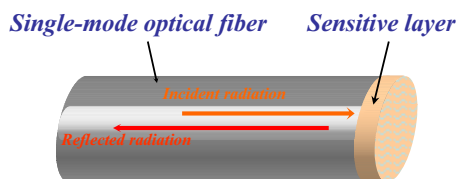


Fig. 1. Schematic view of the Fabry-Perot-based configuration.

First described in 1899 by Fabry and Perot (Fabry & Perot, 1899), the interferometer known by their names makes use of multiple reflections between two closely spaced surfaces. In fact the light is partially reflected each time it reaches the second surface, resulting in multiple offset beams which can interfere with each other. The amount of light reflected at the first interface can be calculated as the sum of the multiple reflected beams and is strongly influenced even by very small changes of the distance between the two surfaces (the sensitive layer thickness) or its optical properties (the sensitive layer refractive index) (Dakin & Culshaw, 1988). This explains the massive use of such configuration in fiber optic-based sensing in the two past decades, especially for the detection and measurements of various physical, chemical and biomedical parameters (Jackson, 1994; Chan et al., 1994). All



these characteristics, combined with the possibility of integrating a number of sensitive materials with the optical fibers by means of very simple, low cost and versatile deposition techniques make it one of the most attractive and useful optoelectronic configuration especially suitable for practical applications.

The principle of operation of an optoelectronic sensor in reflectometric configuration relies thus on the fact that a modulation of the intensity of light reflected at the fiber-sensing overlay interface occurs due to changes in layer thickness ( $d_{film}$ ) and complex refractive index ( $\tilde{n}_{film}$ ). As matter of fact the fiber-film reflectance can be expressed as (Macleod, 2001):

$$R = \left| \frac{r_{12} + r_{23} \cdot e^{-i \cdot \tilde{k}_{film}}}{1 + r_{12} \cdot r_{23} \cdot e^{-i \cdot \tilde{k}_{film}}} \right|^2 \quad (1)$$

with:

$$r_{12} = \frac{n_f - \tilde{n}_{film}}{n_f + \tilde{n}_{film}}; r_{23} = \frac{\tilde{n}_{film} - n_{ext}}{\tilde{n}_{film} + n_{ext}} \quad (2)$$

$$\tilde{k}_{film} = \frac{2\pi \cdot (2 \cdot \tilde{n}_{film} \cdot d_{film})}{\lambda} = \frac{4\pi \cdot n \cdot d_{film}}{\lambda} - i \frac{4\pi \cdot k \cdot d_{film}}{\lambda} = \beta_{film} - i\alpha \cdot d_{film}$$

where  $\tilde{n}_{film} = n - i \cdot k$ ,  $\alpha = 4\pi k / \lambda$  is the overlay absorption coefficient,  $n_f$  and  $n_{ext}$  are the optical fiber and external medium refractive index, and  $\lambda$  is the optical wavelength. Thus, the reflectance changes due to the chemical interaction between sensing overlay and target analyte can be expressed as follows:

$$\Delta R = \left( \frac{\partial R}{\partial n} \right) \cdot \Delta n + \left( \frac{\partial R}{\partial \alpha} \right) \cdot \Delta \alpha + \left( \frac{\partial R}{\partial d_{film}} \right) \cdot \Delta d_{film} = S_n \cdot \Delta n + S_\alpha \cdot \Delta \alpha + S_d \cdot \Delta d_{film} \quad (3)$$

where  $S_n$ ,  $S_\alpha$  and  $S_d$  are the sensitivities against the variations of the effective refractive index, the absorption coefficient and the overlay thickness, respectively. They strongly depend upon the geometrical and electro-optical properties of the sensitive nanocoatings and upon the environmental condition (for example vapor or liquid phase), and for this reason they have to be properly considered case by case. In particular, several effects could be involved to promote a reflectance change as a consequence of the analyte molecule adsorption within the sensitive overlay: first of all, swelling of the SWCNT nano-composite overlay that leads to a consequent increase of the film thickness; also, refractive index variations are expected due to the film density variation as expressed by the Lorentz-Lorentz law (Kingery et al., 1976). In addition, according to the plasma optic effect (Wooten, 1972; Soref & Bennet, 1987; Heinrich, 1990) a change either in the real part of the refractive index or in the absorption coefficient could be possible as a consequence of the free carrier concentration change induced by charge transfer mechanisms during analyte sorption. Modifications of film reflectance could be also possible due to optical absorption changes induced by chemical interaction with target analyte. In addition, it is noteworthy that, when very low chemical concentrations are considered (as in this work), it can be assumed that the analyte molecule adsorption occurs at constant overlay thickness ( $\Delta d_{film} = 0$  in (3)).

### 3.1 Optoelectronic interrogation system

An important issue to address when dealing with sensors is the design and development of a proper demodulation unit able to provide a continuous interrogation of single or multiple sensor probes by minimizing size, complexity and increasing the cost effectiveness. So far, a variety of schemes have been proposed for the interrogation of a fiber optic sensor based on the FP cavity, the most used ones relying on spectrum-modulating approach and single wavelength reflectometry (Kersey & Dandridge, 2001). Here the attention has been focused on this last technique, which is simple to implement and requires just few widespread commercial and low-cost optoelectronic components while preserving excellent performance. In addition it enables the fabrication of cost-effective, reliable, robust and portable equipments, which are factors of crucial importance for in-situ and long-term monitoring applications and for the desired technology transfer to the market. The typical interrogation scheme enabling the reflectance monitoring of a FP cavity realized on the distal end of an optical fiber is shown in Fig. 2 (Consales et al., 2007\_b).

It basically involves a superluminescent light emitting diode (with central wavelength  $\lambda=1310$  nm and a bandwidth of approx. 40 nm), a 2x2 coupler and two photodetectors. It provides an output signal  $I$  that is proportional to the fiber-film interface reflectance  $R$  and that is insensitive to eventual fluctuations of the optical power levels along the whole measurement chain. As matter of fact, emitted light is splitted by the coupler and directed to the sensing probe (where partial reflection occurs) and to the first photoreceiver, whose output thus consists of an electrical signal ( $V_{source}$ ) proportional to the power emitted by the source ( $P_{source}$ ). Reflected light is directed through the coupler to the second photoreceiver which responds with an electrical signal ( $V_{signal}$ ) proportional to  $P_{source}$  and to the overlay reflectance ( $R$ ). The intensity compensation is obtained by considering the ratio between the voltage signals at the two photoreceivers:

$$I = \frac{V_{signal}}{V_{source}} = \alpha \cdot R \quad (4)$$

where  $\alpha$  is a constant accounting for all the set-up parameters. In the followings, the relative change of the sensor output  $\Delta I/I_0$  is considered (where  $I_0$  is the output signal in the reference or initial condition), which, in turn, corresponds to the relative reflectance change occurring at the fiber-sensitive layer interface ( $\Delta R/R_0$ ). Synchronous detection is typically implemented to enhance the system performance, by amplitude modulating the light source at 500 Hz and retrieving the photodetector voltages by using a dual channel lock-in amplifier. The minimum  $\Delta R/R_0$  that can be detected by means of this interrogation system, calculated considering the maximum scattering on the sensor response in a steady-state level for a time interval of at least 10 minutes, is typically in the range  $1-6 \cdot 10^{-4}$ . In addition, a Time Division Multiplexing (TDM) approach is typically exploited to perform the quasi-simultaneous interrogation of up to eight optical probes by means of a fiber optic switch.



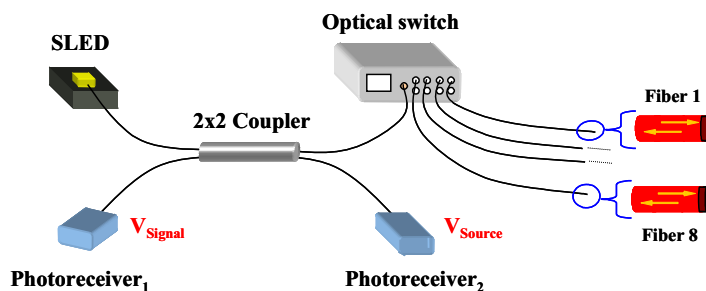


Fig. 2. Schematic illustration of the typical interrogation scheme adopted for the single wavelength reflectance monitoring of an optical cavity realized upon the fiber tip

### 3.2 Opto-chemical sensor fabrication

The realization of thin films of SWCNTs with a controllable thickness is an important basis for the future development of their scientific understanding and technological applications. Proper manipulation techniques are required for applying thin-films of carbon nanotubes on substrates that do not allow direct grow methods. Although various proposals exist for their incorporation into devices, in single tube or thin film architectures (Bachtold et al., 2001), here the Langmuir Blodgett (LB) technique has been chosen as way to transfer nanometer-scale layers of SWCNTs upon either bare optical fibers or Cadmium Arachidate (CdA) buffer-linker material, previously deposited (by the same technique) upon the fiber end in order to improve the carbon nanotubes adhesion on the sensors surface. The CdA has been chosen as buffer material due to its peculiar amphiphilic molecular structure suitable for LB deposition process (Takamoto et al., 2001; Di Luccio et al., 2004).

The LB-technique is one of the most promising techniques for preparing such thin films as it enables the precise control of the monolayer thickness, homogeneous deposition of the monolayer over large areas and the possibility of making multilayer structures with varying layer composition (Roberts, 1990). An additional advantage of the LB technique is that monolayers can be transferred on almost any kind of solid substrate. However these advantages have to be traded with the low speed of the deposition procedure as well as the limited number of materials suitable for this technique. As represented in Fig. 3, the molecules of the films to deposit are firstly dispersed onto the surface of a sub-phase, typically oriented with the hydrophobic part upwards and with the hydrophilic one immersed in water. Subsequently, a reduction of the surface area occupied by each molecule is performed by means of moving barriers in order to produce a solid phase of a given surface pressure in which the molecules are densely packed forming an highly ordered array (James & Tatam, 2006). From this phase the molecules can be transferred to a properly cleaned and prepared solid substrate by its dipping through the condensed Langmuir layer. As the solid phase is reached only at high surface pressures, a continuous reduction of the moving barriers is performed when the molecules are transferred from the sub-phase to the substrate in order to keep the surface pressure constant, ensuring that the solid phase is maintained. Repeated dipping of the same substrate are also possible, resulting in the deposition of a thin film one monolayer at a time.

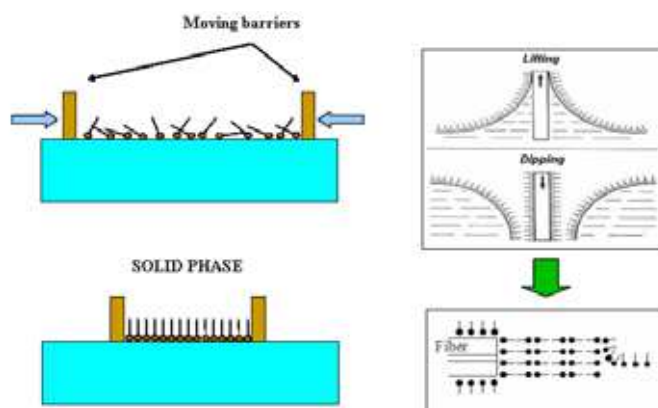


Fig. 3. Schematic representation of the Langmuir-Blodgett deposition procedure.

For CdA buffer multilayer deposition, a solution (0.953 mg/ml) of arachidic acid [ $\text{CH}_3(\text{CH}_2)_{18}\text{COOH}$ ] in chloroform is typically spread onto a sub-phase of deionized water (18 M $\Omega$ ) containing  $10^{-4}$  M cadmium chloride ( $\text{CdCl}_2$ ). The sub-phase pH is kept constant at a value of 6.0, with the temperature fixed at 23°C. The monolayer is compressed with a barrier rate of 15 mm/min up to a surface pressure of 27 mN/m. The single layer is deposited on the SOF with a vertical dipping rate of 12 mm/min. After a proper drying of 24 hours, the coated fiber is ready for the deposition of the CNT sensing layers.

For SWCNT film deposition, a solution (0.2 mg/ml) of SWCNT pristine material in chloroform is spread onto a sub-phase constituted by deionized water (18 M $\Omega$ ) with  $10^{-4}$  M of  $\text{CdCl}_2$ . The sub-phase pH and the temperature are kept constant at values of 6.0 and 23°C, respectively. The monolayer is compressed with a barrier rate of 15 mm/min up to a surface pressure of 45 mN/m. The single layer is deposited on the SOF surface, either bare or already coated by 20 monolayers of CdA (Penza et al., 2005\_b), with a dipping rate of 3 mm/min. After a proper drying of 12 hours overnight, the sensing multilayers deposited are ready for the experimental testing. The raw pristine material of commercial SWCNTs has always been used as-bought, without any purification treatment. The samples are prepared by sonicating SWCNT suspension in chloroform for 1 hour at room temperature prior to the deposition. It is also noteworthy that before the LB deposition procedure the SOFs are previously accurately polished from the acrylic protection and cleaved with a precision cleaver in order to obtain a smooth and plane surface. Then, they are washed in chloroform and dried with gaseous nitrogen to be ready for the deposition. The number of deposited CdA and/or SWCNT monolayers are controlled by choosing how many times the substrate is dipped inside or lifted from the solution containing the monolayer to transfer.

### 3.3 Structural and morphological characterization of SWCNT overlays

The rational design of a chemical sensor and of its performance is something which is possible only if the sensitive material properties and the way they are affected by different deposition parameters or ambient conditions are well known and understood. To this aim an extensive characterization of the as-bought SWCNT powders as well as of the deposited LB SWCNT films has been carried out in order to investigate their structural and

morphological features. Such characterization involved X-ray diffraction (XRD) and Raman Spectroscopy analyses, High-Resolution Transmission Electron Microscopy (HRTEM) and Scanning Electron Microscopy (SEM) observations. In particular, in Fig. 4.a is reported the typical XRD spectrum of as-bought SWCNT powder (1 mg) material. The pattern exhibits a well-defined graphite-like (002) diffraction peak at  $2\theta = 26.5^\circ$ , and a broad band centered at lower  $2\theta = 22^\circ$  from amorphous carbon or non-nanotube carbon material.

Further XRD analyses performed on CdA multilayers on glass substrates evidenced a CdA monolayer spacing of about 2.8 nm for cadmium arachidate. The same measurements, performed with a SWCNT multilayer, revealed a carbon nanotubes monolayer spacing of about 2.0 nm (Penza et al., 2005\_b). Also Raman spectroscopy analyses have been conducted to characterize the fabricated LB films based on SWCNTs already deposited on the SOF tip. To this aim, a Raman microscope functioning in backscattering configuration employing a HeNe laser (633 nm) and 50x and 100x objective lenses was used. The results are shown in Fig. 4.b, where the typical Raman spectrum of a SWCNT film is reported. The characteristic multi-peak feature "G-band" at about  $1580\text{ cm}^{-1}$ , corresponding to carbon atoms vibration tangentially with respect to the nanotube walls (Saito et al., 1998), together with the less remarkable disorder-induced "D-band" peak typically in the range  $1300\text{--}1400\text{ cm}^{-1}$ , representing the degree of defects or dangling bonds, can be easily revealed.

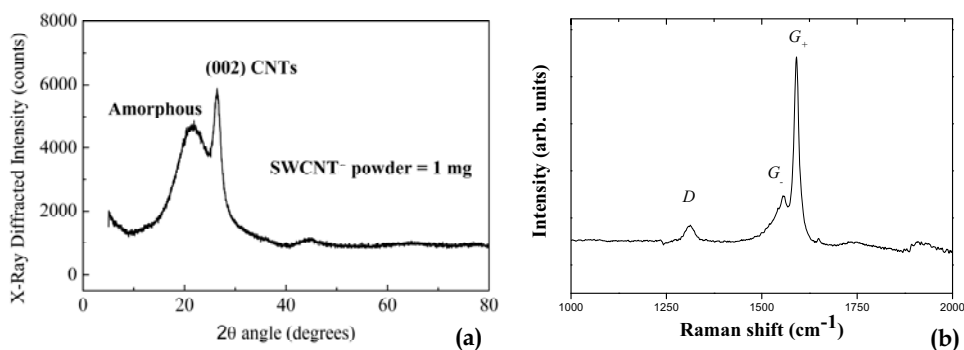


Fig. 4. (a) X-ray diffraction spectrum obtained from HiPco SWCNT powder (1 mg) and (b) typical Raman spectrum of a LB SWCNT film directly deposited on the optical fiber tip.

In particular the observation of the two most intense G peaks (labelled  $G^+$  and  $G^-$ ) confirm the single-walled nature of the carbon tubes while their predominant semiconducting behavior can be derived by the Lorentzian lineshape of the  $G^-$  feature which, on the contrary, is broadened for metallic SWCNTs (Saito et al., 1998). In addition, the large ratio of G to D peaks give us an indication of an ordered structure of the deposited SWCNT overlay. It is worth noting that, since the Raman studies have been performed on SWCNT film already deposited on the fiber end-face, the results shown also confirm their successful integration with optical fiber technology. The HRTEM images of a SWCNT powder, reported in Fig. 5 at (a) low and (b) high magnification, confirm the nanometric dimension of the carbon tubes and reveal the presence between them of some Fe metal particles, a typical catalyst used in the HiPco production process of carbon nanotubes.

Finally, in Fig. 5.c is reported the typical SEM images of CdA-buffered LB SWCNT films deposited upon a SOF tip. It demonstrates once more the success of the integration of carbon nanotubes with the optical fiber and reveals their attitude to adhere one to each other forming bundles or ropes with a spaghetti-like arrangement.

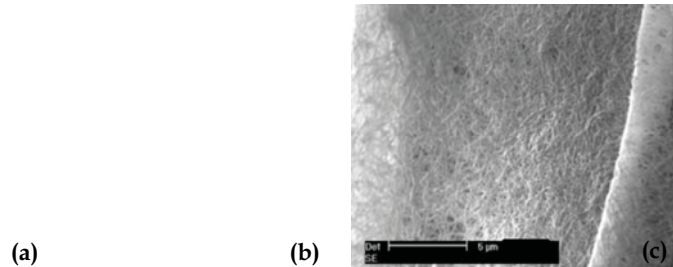


Fig. 5. HRTEM images of SWCNT powder at (a) low and (b) high magnification and (c) SEM images of CdA-buffered SWCNT LB films deposited on a SOF tip.

#### 4. Environmental monitoring applications: Experimental Results

In the following we report the results obtained during the last years of research focused on the development of SWCNTs-based fiber optic chemo-sensors. In particular, we focus our attention on chemical trace detection in air and water, at room temperature. The strong potentiality of this novel SWCNTs-based fiber optic sensing technology to be employed for numerous practical environmental monitoring application is clearly demonstrated.

##### 4.1 Room temperature detection of VOCs in air

The investigation and characterization of the VOC detection performance of SWCNTs-coated opto-chemical sensors has been carried out by means of an experimental setup ad hoc designed and realized, a schematic representation of which is reported in Fig. 6.

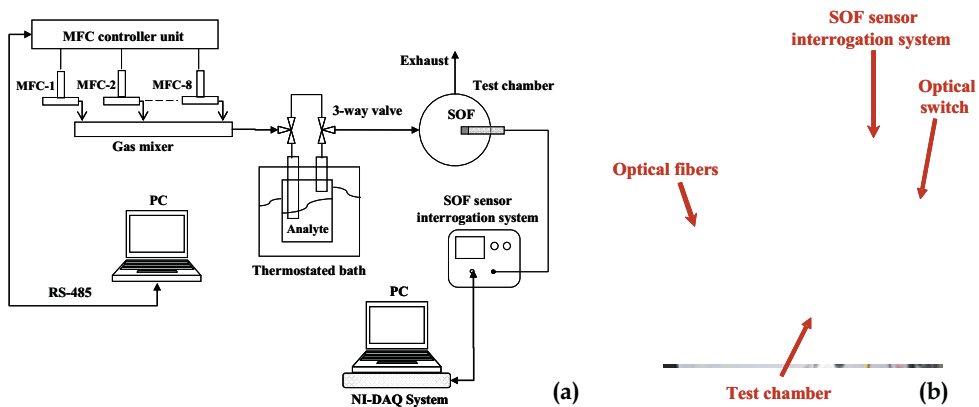


Fig. 6. Experimental setup used for the vapor testing.

In particular the optical fiber probes are located in a properly designed test chamber realized in stainless steel. The volume of the test chamber was 1200 ml, the total flow rate per exposure has been kept constant at 1000 ml/min and the vapors have been generated by the bubbling method. The gas flow rate has been controlled by a mass flow-meter driven by a controller-unit communicating with a PC via standard RS-485 serial bus. The controller unit was able to drive up to eight different gas-channels, and the gas flow rate in each gas-channel was regulated by a dedicated mass flow meter with a full scale of the mass flow ranging from 10 to 1000 ml/min. Numerous tests have been performed by using nitrogen or dry air as reference and carrier gas to transport the generated vapors inside the test ambient: dry air has been chosen because of the higher stability demonstrated by the optical fiber sensor signals. All the experiments have been conducted at room temperature.

The capability of SWCNT overlays of undergoing changes in their complex refractive index and thickness as consequence of the adsorption of target analyte molecules was demonstrated for the first time in 2004 (Penza et al., 2004). In that case LB films consisting of SWCNT bundles were transferred upon the optical fiber tip by using a buffer LB multilayer of CdA pre-deposited on the sensor surface in order to promote the CNT adhesion. The fabricated probes were exploited for the detection of several VOCs, such as isopropanol, methanol, ethanol, toluene and xylene. However, in 2005, multilayers of SWCNTs with different thicknesses were successfully deposited directly upon the optical fiber surface by a modification of the LB process (Consales et al., 2006\_b), resulting in an improvement of the sensing performance of the un-buffered configuration with respect to the buffered case, especially in term of sensor sensitivity. As an example, Fig. 7 shows the highest  $\Delta R/R_0$  exhibited by a fiber optic probe coated with 4 SWCNT monolayers (namely SOF-4) when exposed to 30-minutes decreasing concentration pulses of xylene vapors with respect to the counterpart optoelectronic sensor arranged in the CdA buffered configuration (2 monolayers of SWCNTs deposited onto 20 monolayers of CdA). In both cases, significant reflectance changes occurred on analyte exposure as consequence of the variation in the SWCNT overlay refractive index promoted by toluene molecules adsorption.

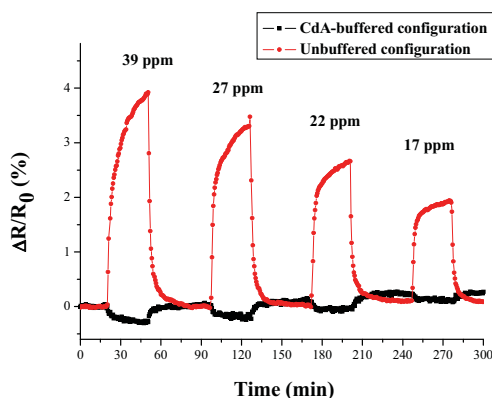


Fig. 7.  $\Delta R/R_0$  occurred on xylene vapor exposure to CdA-buffered and un-buffered SWCNTs-based opto-chemical sensors, at room temperature.

Both sensors exhibited the capability of detecting the chemical under investigation at ppm traces combined with fast response, complete reversibility (enabling the reuse of the sensor after a given measurement) and a marked response time dependence on analyte concentration. However the sensor SOF-4 provided response changes more than one order of magnitude higher than the ones provided by the counterpart probe in the CdA-buffered configuration. In light of this results, strong interest was devoted to the investigation of the sensing capabilities of SWCNTs-based opto-chemical sensors arranged in the un-buffered configuration against several VOCs.

In Fig. 8.a are reported the results of toluene vapor testing carried out by exposing the probe SOF-4 to four toluene pulses with concentration in the range 54-93 ppm. The results obtained confirmed the behavior of the fiber optic sensor exhibited during xylene testing: as matter of fact, also in this case a  $\Delta R/R_0$  increase on exposure was observed as consequence of analyte molecule adsorption. A less pronounced dependence of the response time on toluene concentration was noticed, revealing that different adsorption dynamics occur depending on the VOC under investigation. Also, a slight drift in the signal baseline can be recognized, due to little thermal changes in the not perfectly thermo-stated test chamber.

In order to investigate the reliability of the proposed transducers, a repeatability test has been carried out for the same fiber optic sensor. The results are shown in Fig. 8.b, where the  $\Delta R/R_0$  occurred as consequence of two xylene exposures at 21 ppm are reported. As evident, the opto-chemical probe demonstrated high repeatability and reliability also at very low analyte concentrations.

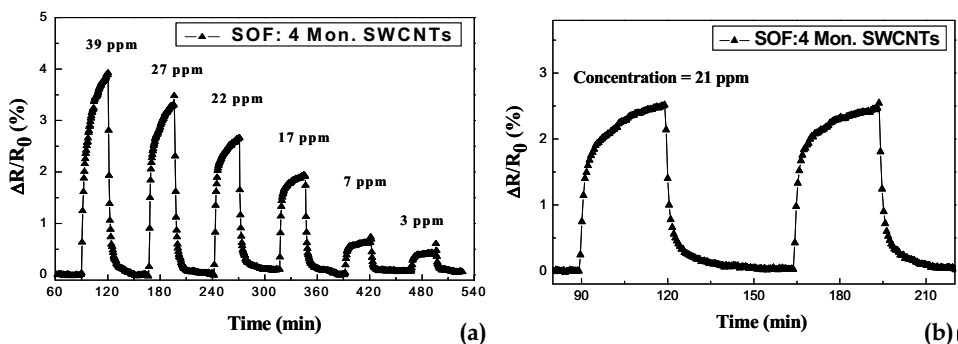


Fig. 8. (a) Response of sensor SOF-4 to toluene vapors at room temperature and (b) repeatability test performed exposing the same sensor to 2 pulses of xylene vapors (21 ppm).

These results have to be considered at constant temperature, because no thermal variation occurred meanwhile. However it is evident that monitoring of thermal drifts and compensation of their effects on sensor response are strictly required to not affect the system performance. Temperature monitoring could be implemented by means of proper fiber bragg grating temperature sensors, which could be either separately inserted within the test ambient or integrated with the optical fiber probe (Cusano et al., 2004). Similarly, CNTs-based fiber optic chemo-sensors demonstrated a relevant sensitivity also to humidity changes (Consales et al., 2006\_b), thus revealing the necessity of proper calibrations and compensations of the sensor response, especially when high accuracy is requested.



In Fig. 9 have been reported the calibration curves of sensor SOF-4 obtained against toluene and xylene vapors, which revealed an almost linear behavior in the investigated concentration ranges. In addition, by comparing sensor sensitivities to both analytes, calculated as relative reflectance change upon concentration unit ( $S_{analyte}=(\Delta R/R_0)/C$ ) (D'Amico & Di Natale, 2001) a SOF sensitivity to xylene ( $S_{xylene}=1.1 \cdot 10^{-3} \text{ ppm}^{-1}$ ) more than two times higher than that to toluene ( $S_{toluene}=4.7 \cdot 10^{-4} \text{ ppm}^{-1}$ ) has been found. Considering the minimum  $\Delta R/R_0$  achievable with the exploited interrogation unit, a resolution of approx. 290 ppb and 120 ppb have been estimated for toluene and xylene, respectively.

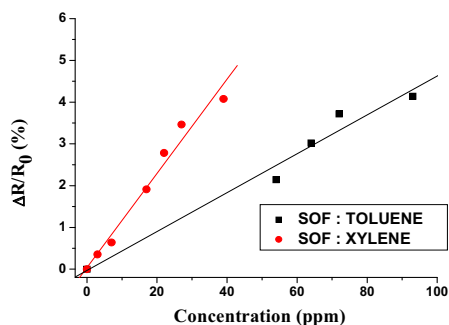


Fig. 9. Calibration curves of sensor SOF-4, exposed to toluene and xylene vapors.

This excellent resolutions are more than three orders of magnitude higher than that obtained by means of a fluorosiloxane polymer-based Surface Plasmon Resonance (SPR) optical fiber sensor (900 ppm and 190 ppm, respectively for toluene and xylene) (Abdelghani & Jaffrezic-Renault, 2001), and more than two orders of magnitude higher than that provided by a multimodal optical fiber sensor sensitized by phenyl-modified porous silica (100 ppm and 20 ppm, respectively) (Abdelmalek et al., 1999).

#### 4.1.1 Influence of monolayers number and CdA buffer on sensor sensitivity

Here, the influence of the number of SWCNT monolayers on the sensor performance are discussed. The differences between the sensing capability of buffered and un-buffered configurations are also better discussed. To this aim, four opto-chemical sensors coated by different numbers of monolayers, directly deposited on bare substrates and also buffered by 20 LB monolayers of CdA, have been simultaneously exposed to toluene and xylene vapors. Fig. 10.a reports the  $\Delta R/R_0$  versus toluene concentration for all the tested sensors. It can be seen that a sensitivity increase has been obtained by passing from 2 ( $0.9 \cdot 10^{-4} \text{ ppm}^{-1}$ ) to 4 SWCNT monolayers ( $4.7 \cdot 10^{-4} \text{ ppm}^{-1}$ ). On the contrary, the optical chemo-sensor coated by a higher number of monolayers (12), and thus by a thicker SWCNT film, exhibited a negative sensitivity ( $-0.7 \cdot 10^{-4} \text{ ppm}^{-1}$ ). This means that for this sensor the fiber-film interface reflectance decreases on exposure. This is due to the fact that the film reflectance, and thus also the sensor sensitivity, is strongly dependent on the thickness and refractive index of the CNT overlay, in accordance with (1). As a matter of the fact, depending on the geometric features of the film deposited atop the optical fiber, either positive or negative sensitivities to a target analyte can be obtained.

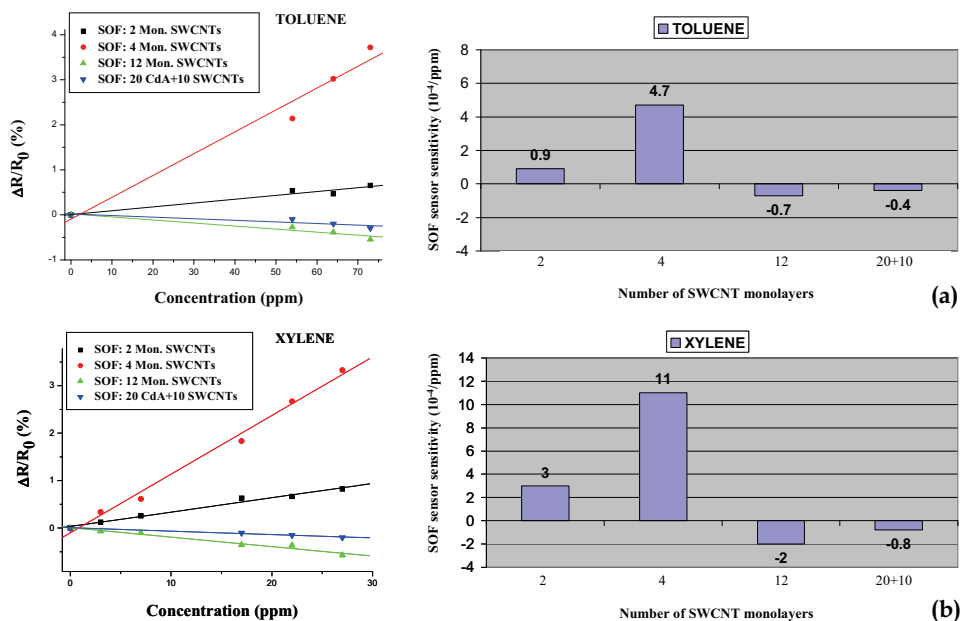


Fig. 10. Calibration curves and sensitivities obtained by exposing four fiber optic sensors coated by a different number of SWCNT monolayers to (a) toluene and (b) xylene vapors.

For the same reason, the CdA buffer multilayer, whose optical properties are quite similar to those of the standard optical fibers, and thus not optimized for the particular configuration exploited, dramatically decreases the sensitivity of optical fiber sensors ( $-0.4 \cdot 10^{-4} \text{ ppm}^{-1}$ ). It is noteworthy, however, that by choosing a buffer-linker material whose optical and geometrical features (such as the multilayer thickness and refractive index) are well optimized for the specific configuration, one could be able to strongly enhance the SOF sensor performance. From Fig. 10.b it can be seen that the four fiber optic chemo-sensors exhibited the same behaviors also in case of xylene vapor testing: hence, it demonstrates that the inversion of the optoelectronic sensor sensitivities is not due to the particular analyte tested, but to the optical configuration exploited. This feature could be very useful for pattern recognition analysis in case of multi-transducer approaches, where complementary sensors are exploited to improve the analyte discrimination (Penza et al., 2005\_b).

#### 4.1.2 Response and recovery time analysis

As the experimental results revealed a dependence of sensor response times (and as consequence of the adsorption/desorption dynamics) on analyte concentration, a detailed analysis of response and recovery times of sensor SOF-4 has been performed (Consales et al., 2007\_b) by its exposure to different concentration pulses of toluene and xylene vapors (the exposure time was 30 minutes). The response (recovery) time has been calculated as the time the output signal needed to pass from 10% to 90% (from 90% to 10%) of the total signal variation. The results obtained for both chemicals are quite similar and revealed the attitude

of response time to increases with analyte concentration while the recovery time is quite constant. In particular, the minimum response time in case of toluene, obtained for 54 ppm, was approx. 7 minutes while the maximum one, obtained for 93 ppm, was approx. 11 minutes. The recovery time was as low as approx. 5 minutes. Slower responses were observed in case of xylene exposure, for which the SOF response times increased from approx. 4 minutes (3 ppm) to approx. 18 minutes (39 ppm), and the recovery time was approx. 6 minutes. This could be ascribed to a different adsorption kinetic of the two analyte molecules inside the CNT sensitive nanocoatings. It is noteworthy, however, that the response times of the proposed fiber optic chemo-sensors are relatively good taking into account the volume of the test chamber and the total flow rate per exposure. It is also important noting that although these times could be reduced by depositing a lower amount of carbon nanotubes on the SOF tip, the choice of the geometric features of the sensitive overlay has to be made by considering the trade-off that exists between sensor sensitivity and response (and recovery) time (Consales et al., 2007\_b).

#### 4.2 Towards fiber optic tongue: chemical trace detection in water

In this section the attention has been focused on the feasibility of exploiting the excellent sensing properties of CNTs for the development of high performance optoelectronic sensors capable of chemical trace detection in aqueous environments, at room temperature.

A schematic view of the experimental setup exploited for chemical trace detection in water is reported in Fig. 11.a. The SWCNTs-based opto-chemical transducers have been inserted in a beaker containing pure water. The presence within the test ambient of the analyte under investigation has been promoted by its injection inside the beaker. The injected volume has been chosen, each time, in order to obtain the desired analyte concentration. The polluted water has been continuously stirred to ensure maximum dispersion of analyte. In addition, after each exposure, the capabilities of SOF sensors to recover the initial steady state level have been investigated by restoring the initial condition of pure water: pure water has been continuously injected in the test chamber, while the contaminated water, previously present in it, contemporarily stilled out.

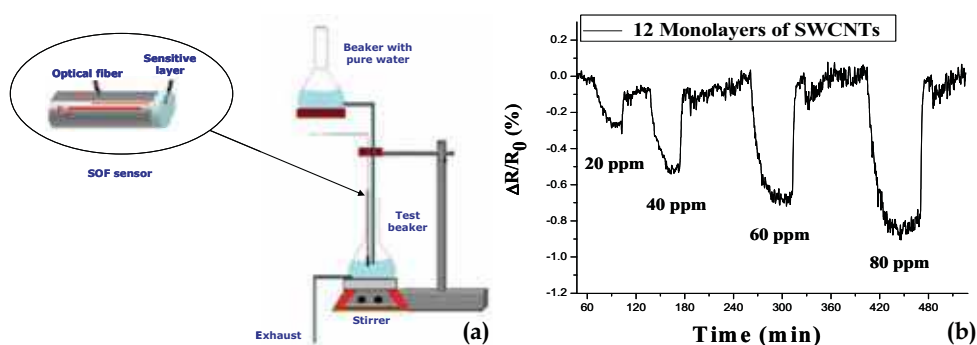


Fig. 11. (a) Experimental setup exploited for chemical trace detection in water and (b)  $\Delta R/R_0$  occurred to the sensor SOF-12 on toluene injections, at room temperature.

## Thank You for previewing this eBook

You can read the full version of this eBook in different formats:

- HTML (Free /Available to everyone)
- PDF / TXT (Available to V.I.P. members. Free Standard members can access up to 5 PDF/TXT eBooks per month each month)
- Epub & Mobipocket (Exclusive to V.I.P. members)

To download this full book, simply select the format you desire below

